

Communication

## Relaxation Rate for an Ultrafast Folding Protein Is Independent of Chemical Denaturant Concentration

Troy Cellmer, Eric R. Henry, Jan Kubelka, James Hofrichter, and William A. Eaton

*J. Am. Chem. Soc.*, 2007, 129 (47), 14564-14565 • DOI: 10.1021/ja0761939

Downloaded from <http://pubs.acs.org> on February 9, 2009



### More About This Article

Additional resources and features associated with this article are available within the HTML version:

- Supporting Information
- Links to the 1 articles that cite this article, as of the time of this article download



**ACS Publications**  
High quality. High impact.

- Access to high resolution figures
- Links to articles and content related to this article
- Copyright permission to reproduce figures and/or text from this article

[View the Full Text HTML](#)



## Relaxation Rate for an Ultrafast Folding Protein Is Independent of Chemical Denaturant Concentration

Troy Cellmer,<sup>†</sup> Eric R. Henry,<sup>†</sup> Jan Kubelka,<sup>‡</sup> James Hofrichter,<sup>†</sup> and William A. Eaton<sup>†</sup>

Laboratory of Chemical Physics, NIDDK, National Institutes of Health, Bethesda, Maryland 20892-0520, and  
Department of Chemistry, University of Wyoming, Laramie, Wyoming 82071

Received August 23, 2007; E-mail: eaton@helix.nih.gov

Single-domain globular proteins composed of less than 100 residues often show simple thermodynamic and kinetic properties with only two populations of molecules, folded and unfolded, present at all times and under all solution conditions.<sup>1</sup> This two-state behavior is characterized by a linear relation between the apparent activation free-energy changes and the concentration of chemical denaturant, resulting in a V-shaped plot of the log-(relaxation rate) vs denaturant concentration, called a “chevron” plot. For a two-state system the relaxation rate is the sum of the folding and unfolding rates ( $k_{\text{obs}} = k_f + k_u$ ), the equilibrium constant is the ratio ( $K_{\text{eq}} = k_u/k_f$ ), and the equilibrium sensitivity to chemical denaturant is related to the two slopes of the chevron plot by:  $m_{\text{eq}} = m_u - m_f$ . The most common chevron plot has linear arms at low and high denaturant concentrations where the relaxation rate corresponds to the folding and unfolding rates, respectively. As in the linear free-energy relations observed in chemical reactions, the relative sensitivity of the folding and unfolding rates resulting from the change in stability is taken as a measure of the position of the transition state along a putative reaction coordinate, in this case the compactness of the structure. There has been much discussion on the interpretation and significance of deviations from linear folding and unfolding arms to chevron plots (see excellent review by Oliveberg and Wolynes<sup>2</sup>). Several factors have been suggested as causes for this deviation, including the presence of intermediate states, a change in the relative position of the transition and denatured states with changing solvent or mutation, and the presence of parallel pathways. Most recently, the slopes of chevron plots were used by Muñoz and co-workers to make quantitative estimates of the free-energy barrier heights separating folded and unfolded states.<sup>3</sup> Using an idealized free-energy surface, they conclude that chevron plots flatter than predicted from the equilibrium experiments ( $m_{\text{eq}} = m_u - m_f$ ) are a sign of marginal folding barriers. Fersht and co-workers have made qualitative arguments to suggest that relatively flat chevron plots are expected for barrierless folding.<sup>4</sup>

Here we address the connection between free-energy surfaces and chevron plots in a kinetic study of an ultrafast folding protein, the 35-residue subdomain from the villin headpiece.<sup>5</sup> The denaturant-induced unfolding curves, measured by circular dichroism and fluorescence, are typical for small single domain proteins and are well fit assuming a two-state thermodynamic model (Figure 1). The kinetics, however, are strikingly different from what is observed for slower folding two-state proteins; there is no measurable dependence of the relaxation rate on denaturant concentration (Figure 2). The flat chevron plot indicates a clear deviation from classical two-state behavior.<sup>3</sup>

If the folding and unfolding rates are calculated from relaxation rates and the equilibrium constants derived from the fits in Figure 1, the logarithm of the folding and unfolding rates are nonlinear

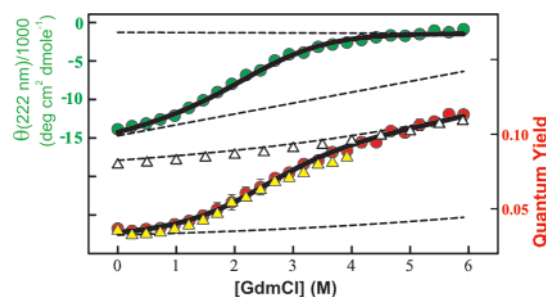


**Figure 1.** Guanidinium chloride (GdmCl) induced unfolding curve measured by CD and tryptophan fluorescence quantum yield (pH 4.9, 40 °C). The triangles are the amplitudes from kinetic measurements. The data were fit with a two-state model (see Supporting Information), yielding  $c_m = 2.44$  M, and  $m = 0.82$  kcal mol<sup>-1</sup> M<sup>-1</sup>.

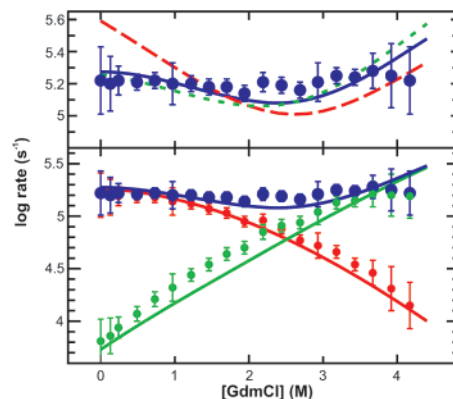


**Figure 2.** Kinetics. (a) Measured relaxation rates following laser T-jump to 40 °C (blue points). Rates were calculated from theoretical free energy surfaces (Figure 3) assuming no denaturant (D) or reaction coordinate (R.C.) dependence in the hopping rate parameter,  $\gamma$  (long-dashed red curve); D-dependence only,  $\gamma = \gamma_0(1 + \alpha[\text{GdmCl}])$  (short dashed green curve,  $\alpha = 0.63$ ); and both D- and R.C.-dependence,  $\gamma = \gamma_0(1 + \alpha[\text{GdmCl}])(\exp(-\beta(P - 5)))$  for  $P > 5$  ( $\alpha = 0.63$ ,  $\beta = 0.1$ , continuous blue curve) (see Supporting Information). (b) Folding (red points) and unfolding rates (green points) calculated using a two-state model; folding (red curves) and unfolding (green curves) calculated from Ising-like model with both D- and R.C.-dependent  $\gamma$ .

functions of the denaturant concentration, and resemble those of protein U1A measured by Oliveberg and co-workers.<sup>6</sup> These nonlinearities were interpreted as a consequence of transition-state movement toward the folded state with increasing denaturant;<sup>6</sup> the equivalent of Hammond behavior in physical organic chemistry.<sup>1</sup> However, the relaxation rate decreases by a factor of  $\sim 300$  between 0 and 4 M GdmCl. In contrast, we observe a relaxation rate that is denaturant independent, and therefore our result requires a different interpretation.

<sup>†</sup> National Institutes of Health.

<sup>‡</sup> University of Wyoming.

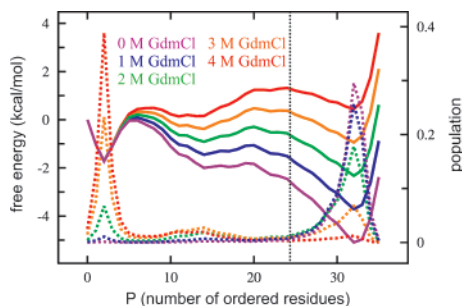


**Figure 3.** Theoretical model. Free energy (continuous curves) and corresponding populations (dashed curves) versus number of ordered residues at various denaturant concentrations from an Ising-like model. The two adjustable parameters of the model, the energy of an inter-residue contact ( $0.65 \text{ kcal mol}^{-1}$ ) and the entropy loss associated with ordering a residue in its native conformation ( $-3.8 \text{ cal mol}^{-1} \text{ deg}^{-1}$ ), were obtained by optimizing the fit to the measured excess heat capacity versus temperature.<sup>9</sup> All species to the right of vertical dotted line are considered part of the folded state, and all to the left are considered the unfolded state.

To understand the denaturant-independent relaxation rates, we have used an Ising-like model as a guide. The model has been described in detail elsewhere,<sup>7–9</sup> so we only present the basic ideas. Each residue of the polypeptide chain exists in one of two possible states, native ( $n$ ) or non-native ( $c$ ). To greatly reduce the number of possible configurations, we employed the double-sequence approximation, in which no more than two continuous stretches of native residues are allowed in each molecule (e.g., ...*cnnc-cnnc*...). The model only allows contacts between residues within a native stretch of residues or between residues in two different native segments, thereby connecting them with a disordered loop. We employed the simplest description of interactions. Non-native interactions and amino-acid type were ignored, with identical energies for all contacts in the known three-dimensional structure (defined as residues with  $\alpha$  carbons separated by less than  $0.8 \text{ nm}$ ) and the same conformational entropy loss for every residue upon ordering it in its native conformation. The effect of denaturant was simulated by reducing the contact energy linearly with GdmCl concentration. The kinetics of folding and unfolding were calculated by hopping along the one-dimensional free-energy surface generated from the partition function (Figure 3), with the fraction of native contacts or number of ordered residues as a reaction coordinate. The simplest assumption that mimics diffusion on the free-energy profile invokes a linear free-energy relation between hopping-rate coefficients and equilibrium constants for adjacent values of the reaction coordinate.

Figure 3 shows the free-energy profiles and the corresponding populations generated by the model as a function of denaturant concentration. Both the profiles and the nearly perfect exponential time course of the calculated fluorescence relaxation (see Supporting Information) are consistent with an approximately two-state process with a small barrier separating the folded and unfolded states.<sup>9</sup> The model predicts a large movement of the major barrier from  $P = 6$  at low denaturant concentration to  $P = 24$  at high denaturant (Figure 3.), but yields a chevron-like, albeit weak, denaturant dependence in contrast to the experimental observation (Figure 2a). However, two significant physical effects were not included in the model. One is based on the elegant single molecule experiments of Schuler and co-workers which show a strong and linear denaturant dependence of the end-to-end diffusion coefficient of the denatured state of a 66-residue cold shock protein.<sup>10</sup> This diffusion coefficient is proportional to the hopping rate on a free energy surface,<sup>11</sup> which

we used to calculate the relaxation kinetics. N. Socci (personal communication), moreover, has shown that the decay time for the end-to-end distance correlation function of the denatured state of a lattice model<sup>12</sup> is nearly the same as that for the correlation time for motion on the reaction coordinate (in this case, the fraction of native contacts,  $Q$ ). Incorporation of the Schuler result markedly reduces the denaturant dependence (Figure 2a).

A second effect, discussed by Wolynes and co-workers,<sup>13,14</sup> is the dependence of the diffusion coefficient on reaction coordinate. As the protein becomes more compact in progressing toward the native state, the diffusion coefficient is expected to decrease. For high barriers a reaction coordinate-dependent diffusion coefficient has no effect on the rate of barrier crossing because only the diffusion coefficient at the barrier top contributes to the rate.<sup>15</sup> In the present case, however, the barriers are very low and move with denaturant concentration. From simulations of lattice models, Wang and co-workers found large decreases in the diffusion coefficient along the  $Q$  coordinate.<sup>16</sup> By introducing a reaction coordinate-dependent hopping rate which decreases exponentially, we find that calculated relaxation rates show less denaturant dependence and the time course remains exponential (see Supporting Information).

We see that a nearly denaturant-invariant, unfolding/refolding relaxation rate can be produced by a large movement of a small free-energy barrier, together with a denaturant and reaction coordinate-dependent diffusion coefficient. We have not considered the possibility that denaturant dependence of the diffusion coefficient may also vary along the reaction coordinate. Nevertheless, we find that the denaturant independence of the kinetics of this ultrafast folding protein can be explained with a simple statistical-mechanical model that yields a marginal folding barrier, approximately two-state thermodynamics, and exponential relaxation kinetics. Although barrierless folding should result in little denaturant dependence,<sup>4</sup> the converse is not necessarily true.

**Acknowledgment.** This research was supported by the Intramural Research Program of NIDDK, NIH. We thank Wai-Ming Yau for peptide synthesis.

**Supporting Information Available:** Details of experimental procedures and theoretical calculations. This material is available free of charge via the Internet at <http://pubs.acs.org>.

## References

- (1) Fersht, A. *Structure and Mechanism in Protein Science*; W. H. Freeman: New York, 1999.
- (2) Oliveberg, M.; Wolynes, P. G. *Quart. Rev. Biophys.* **2005**, *38*, 245–288.
- (3) Naganathan, A. N.; Doshi, U.; Muñoz, V. *J. Am. Chem. Soc.* **2007**, *129*, 5673–5682.
- (4) Huang, F.; Sato, S.; Sharpe, T. D.; Ying, L. M.; Fersht, A. R. *Proc. Natl. Acad. Sci. U.S.A.* **2007**, *104*, 123–127.
- (5) Kubelka, J.; Eaton, W. A.; Hofrichter, J. *J. Mol. Biol.* **2003**, *329*, 625–630.
- (6) Otzen, D. E.; Kristensen, O.; Proctor, M.; Oliveberg, M. *Biochemistry* **1999**, *38*, 6499–6511.
- (7) Muñoz, V.; Eaton, W. A. *Proc. Natl. Acad. Sci. U.S.A.* **1999**, *96*, 11311–11316.
- (8) Henry, E. R.; Eaton, W. A. *Chem. Phys.* **2004**, *307*, 163–185.
- (9) Godoy-Ruiz, R.; Henry, E. R.; Kubelka, J.; Hofrichter, J.; Muñoz, V.; Sanchez-Ruiz, J. M.; Eaton, W. A. *J. Phys. Chem. B* **2007**, in press.
- (10) Nettels, D.; Gopich, I. V.; Hoffmann, A.; Schuler, B. *Proc. Natl. Acad. Sci. U.S.A.* **2007**, *104*, 2655–2660.
- (11) Bicout, D. J.; Szabo, A. *J. Chem. Phys.* **1998**, *109*, 2325–2338.
- (12) Socci, N. D.; Onuchic, J. N.; Wolynes, P. G. *J. Chem. Phys.* **1996**, *104*, 5860–5868.
- (13) Bryngelson, J. D.; Wolynes, P. G. *J. Phys. Chem.* **1989**, *93*, 6902–6915.
- (14) Plotkin, S. S.; Wolynes, P. G. *Phys. Rev. Lett.* **1998**, *80*, 5015–5018.
- (15) Kramers, H. A. *Physica* **1940**, *7*, 284–304.
- (16) Chahine, J.; Oliveira, R. J.; Leite, V. B.; Wang, J. *Proc. Natl. Acad. Sci. U.S.A.* **2007**, *104*, 14646–14651.

JA0761939